Field mapping of buried faults – a new approach applied in the Western Carpathians

František MARKO[1, *], Marian DYDA[2], Vojtech GAJDOŠ[3], Kamil ROZIMANT[3] and Andrej MOJZEŠ[3]

[1] Comenius University, Faculty of Sciences, Department of Geology and Paleontology, Mlynská dolina G, 842 15 Bratislava, Slovakia

[2] Comenius University, Faculty of Sciences, Department of Mineralogy and Petrology, Mlynská dolina G, 842 15 Bratislava, Slovakia

[3] Comenius University, Faculty of Sciences, Department of Applied and Environmental Geophysics, Mlynská dolina G, 842 15 Bratislava, Slovakia

A fault array in an area covered by Quaternary sediments and deprived of bedrock outcrops was investigated using fault trace mapping by geophysical methods and feedback information from dowsing. Brittle structures of the study area are dominated by an ENE–WSW-trending fault zone affecting regional-scale folds and thrusts. The fault network was approximated by dowsing-enhanced mapping and subsequently confirmed by field geophysical measurements using electromagnetic and radon emanometry methods. A resultant detailed map of structural discontinuities highlighted that combined dowsing and geophysical survey is an effective and reliable tool to identify buried faults. This approach with its low costs and fast field recognition is highly recommended for construction-work planning and for exploration and exploitation of mineral resources.

Key words: faults, geophysical survey, dowsing, Western Carpathians.

INTRODUCTION

Classical methods of geological mapping are not much helpful in detecting fault traces buried under a young sedimentary cover in areas where bedrock outcrops are lacking. Our paper describes a simple, fast and effective method of mapping faults in such situations. This new method provides precise and detailed data on fault arrays. Our approach profits from the combination of exact geophysical survey and dowsing. The latter is a poorly understood ability of the human body to detect underground objects and phenomena. Although dowsing is in general officially avoided in the scientific community because of the difficulties encountered in explaining its physical principles (Kowalski, 1996; Fiddick, 2011), many pragmatic field scientists, especially geologists, archaeologists and geophysicists use it for rapid indication of underground objects (Lohmann, 1998; Moldovan et al., 2013). We have successfully incorporated dowsing as a complementary method in water and ore prospecting (Marko et al., 2006; Dyda and Marko, 2010 – unpublished report) and this methodology has also been used by, e.g., Betz (1995) and Landa and Kovalevsky (1997). Therefore, we have confidently applied this technique in our fault trace-

mapping research. During our research on fault tectonics of the investigated brittle shear zone, we tested the dowsing procedure on the known fault strikes. In initial research, we expected geophysical confirmation and localization of the Dúbrava fault described by Marko et al. (1990), but no longer exposed because of advanced mining front and reclamation of the former exploitation pit. Our results were noteworthy. Mapping by dowsing confirmed the occurrence, and detected the trace of the known Dúbrava fault, and, moreover, made it possible to detect and to compile a map of other discontinuities, previously not recorded in the area. This map of discontinuities allowed us to locate appropriate geophysical profiles. Geophysical measurements subsequently made along those profiles confirmed most of the dowsing indications, and helped to explain the nature of the discontinuities.

GEOLOGICAL SETTING

The study area is situated at the northwestern periphery of the Malé Karpaty Mountains in the southernmost part of the Buková furrow. The latter unit, filled with Paleogene sediments (Fig. 1), is superimposed on the northern part of the Malé Karpaty Mts. composed of the Mesozoic cover and nappe units. The area is crossed by a regional-scale brittle shear zone representing the southern boundary of the so-called Carpathian Shear Corridor (CSC), a regional-scale feature described by Marko (2012) and Marko et al. (2013). The CSC is an ENE–WSW-trending Cenozoic strike-slip zone rimmed by the

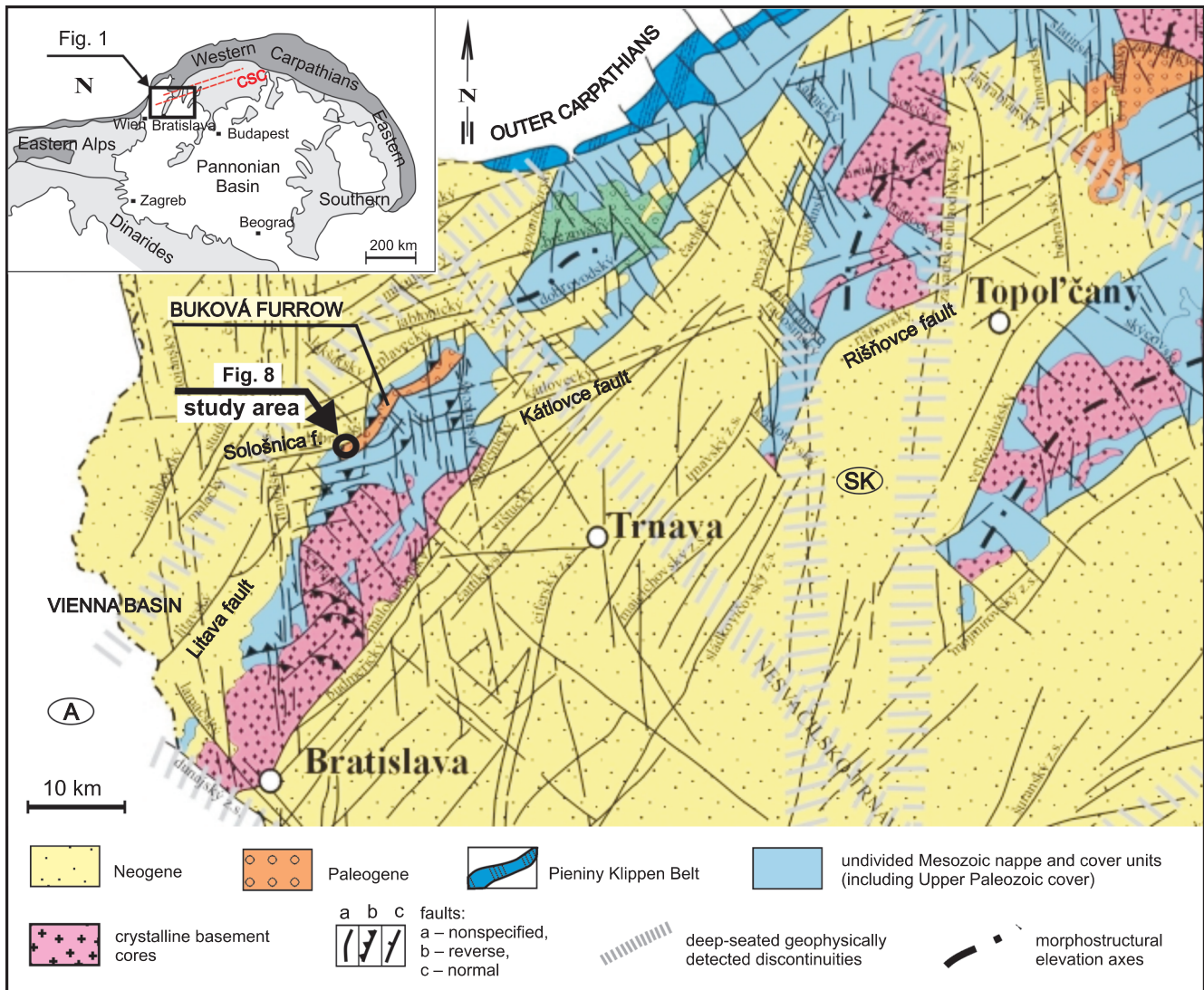* Corresponding author, e-mail: marko@fns.uniba.sk

Fig. 1. Simplified geological map of the westernmost Carpathians showing location of the study area

CSC – Carpathian shear corridor; A – Austria, SK – Slovakia

Myjava and Hron morpholineaments (*sensu* Janků et al., 1984; Pospíšil et al., 1986), and rejuvenating steepened thrust boundaries between the Mesozoic nappe units of the Malé Karpaty Mts. as strike-slip and oblique-slip shear zones in the Neoalpine period. This structural style was noted by Maheľ et al. (1967), Maheľ (1969) and Michalík (1984), and confirmed by Plašienka (1990) and Marko et al. (1990). The mapped polygon is located on the tectonic contact between the Paleogene fill of the Buková furrow and the Neogene fill of the Vienna Basin. The mapped area is completely covered with Quaternary weathering products, and natural bedrock outcrops are lacking.

In this study, we have mapped a fault array in the surrounds of the Hrabník excavation pit near the village of Sološnica. This area has the advantage of good previous knowledge on local geology and tectonics gained by structural observations and field research a few decades ago (Marko et al., 1990 and unpublished research report). Knowledge also accumulated on the later open-mine-front advancing to the south (Marko and Kováč, 1997) and highlighted in the latest geological map by Polák et al. (2011, 2012). The exploitation pit was the key outcrop for localization of observed faults. In 1988, this was a unique outcrop where a large map-scale fault in the CSC southern boundary fault zone was exhumed approximately 150 m along its strike. This sub-vertical NE–SW-striking fault with an almost 1.5 m thick fault damage zone, named the Dúbrava fault, formed a tectonic contact between the Vienna Basin Pannonian sediments and the Uppermost Paleogene – Kiscellian Hrabník Formation of the Buková furrow (see Fig. 9A for comparison; Marko et al., 1990). The sedimentary fill of the Buková furrow (calcarenite layers intercalated with poorly indurated claystones) is strongly folded and faulted near the Dúbrava fault. The excavation front moved to the south, which was accompanied by reclamation of the exploited mining areas; so the Dúbrava fault is no longer exposed. Several minor faults used as testing structures for dowsing and geophysical survey were exhumed at the current mining face.

METHODS

The area around the Hrabník mining pit lacks outcrops, and it is a rural, cultivated terrain used for agriculture. The bedrock and fault structures are covered by the soil horizon and Quaternary weathering products. Without drilling, only indirect methods of geophysical measurement and/or dowsing could be employed to map this fault array.

We originally intended to perform a geophysical survey of the known portion of the Dúbrava fault exhumed at the Hrabník pit and to use geophysical profiles to confirm its continuation on both sides. However, we quickly established that dowsing proved a successful supporting field-work method. This simple procedure was very effective and precise for recording fault intersections with the surface; even those hidden under the Quaternary cover. Dowsing enabled us to map fault strikes and intersecting fault offsets more precisely and rapidly than other alternative methods.

This approach brought quick and precise information on discontinuity traces that were suspected fault structures. Thus, we gained appropriate data to compile the structural map of discontinuities. We were then able to assess optimal orientation and localization of geophysical profiles crossing expected active zones – discontinuities. This geophysical profiling across expected physical discontinuities led to the construction of a map of the distribution of faults. Geophysical profiles were measured during field work between 2011 and 2013, and the course, length and localization of the profiles resulted from a compromise between our needs and terrain possibilities.

GEOPHYSICAL METHODS

Although conductivity via grounded electrodes is usually employed in electrical resistivity mapping, electromagnetic principles provide a more simple and less time-consuming method. Appropriate available instrument methods that detect physical field discontinuities were applied herein. These include electric resistivity and radon emanation. Two relevant methods were applied to localize expected fault traces in the studied field: dipole electromagnetic profiling (DEMP) and soil radon emanometry. Geophysical measurements were made along single profiles situated according to reconnaissance dowsing mapping and, if possible, perpendicular to expected discontinuities. The measuring point spacing on survey lines varied from 5 to 10 m.

Dipole electromagnetic profiling (DEMP) employs a low-frequency electromagnetic field propagated to the rock environment without any direct contact with the Earth's surface. The rock response is measured by track horizontal resistivity changes. This instrument measures electrical conductivity by induced electric currents in the rock environment, and the secondary magnetic field generated by the induced currents. The propagation depth is a combined function of instrument coil spacing and orientation, the employed transmitter frequency and electrical ground conductivity. The depth normally varies from 1.5 to 7 m and we obtained the depth change information using several receiving coils. This relatively simple and fast method allows determination of rock resistivity contrasts.

The *CMD-Explorer* device produced by GF Instruments (CZ), with three receiving coils and penetration depths of 2.2, 4.2 and 6.7 m was used, and the DEMP profiling results are presented in Figures 2–4.

Radon emanometry is an atmogeochemical survey method based on measuring alpha activity in soil air samples from individual depths of rock, weathering cover and soil. This activity results from alpha disintegration processes in the nuclei of radon isotope ^{222}Rn and its daughter products. The parent radium isotope ^{226}Ra commonly occurs in rock foundations and ^{222}Rn is a gaseous element. The fault system is a very appropriate structure for upward movement for both radon and other Earth gases. Therefore, volume activity of the soil's radon gas along the profile crossing the assumed fault zone, measured in kilobecquerels per cubic metre (kBq $\cdot$ m^{-3}), contributes significantly to its location (Gruntorád and Mazáč, 1994; Giammanco et al., 2009).

Radon measurements were performed on sampling from approximately 0.8 m by a portable radon detector *LUK-3R* (SMM, CZ). The results from Radon emanometry profiling are presented in Figure 5.

UNCONVENTIONAL METHODS

Having positive experiences with dowsing in several other field projects focused at groundwater and ore bodies survey, we used the possibility to apply this swift and pragmatic method within the investigated area. We profited a lot from the ability of dowsing to identify structural anomalies, including faults undetectable by other simple methods due to the Quaternary cover in the mapped area.

Human response to energy field changes. This technique, generally known as the dowsing method (DM), is based on not well-defined physical phenomena and properties of water-bearing rocks. Dowsing, as a means of accessing information, is considered here to be a "biofeedback" response based on the interaction of the human organism with its surrounds.

Physical fields on the Earth surface are affected by factors including discontinuities, groundwater hydrodynamics, ore bodies and various anthropogenic creations. A sensitive person can subconsciously detect changes in physical fields caused by hidden underground structures, such as water-filled faults, conductive dikes and other discontinuities. Many ore and mineral deposits were recognized in cultured medieval areas, and their localization had been determined by dowsing (as in Born, 1774; Grecula et al., 2006; Daynes, 2012).

Specific signals received by a trained human allow identification of field discontinuities caused by material differences in physical properties. The nature of physical fields to which the human body is sensitive is still unclear, but it is accepted that sensitivity emanates at least from electromagnetic, magnetic and gravitational energy fields. Signals may also have a visible nature, as sensing is mediated by a pendulum or a dowsing rod; or they may be invisible as heat radiation, warming effects, energy drawing or by elevated emotional awareness through subconscious intuition. Human mental and body effects and nervous system reactions to these stimuli are currently poorly understood. Discrete DM observation principles remain unchanged but currently it has not been clearly explained how our bodies substitute for measuring devices in human feedback systems.

In our research of structural geological phenomena, we assumed a purely pragmatic approach to the problem and a simple dowsing mapping (DM) method was developed for detecting and mapping traces of discontinuities at the topographic surface. A dowser drifted across the study area, constantly recording the received signals. DM techniques are mainly subjective because individual operators employ distinctive methodologies. We used two angled metal rods for detection. The detected discontinuities were referred to as DM faults, and DM points were recorded at anomaly sites, where one or both rods had begun to rotate. This happened at DM route intersections with rock discontinuities. After crossing a discontinuity, the rods'
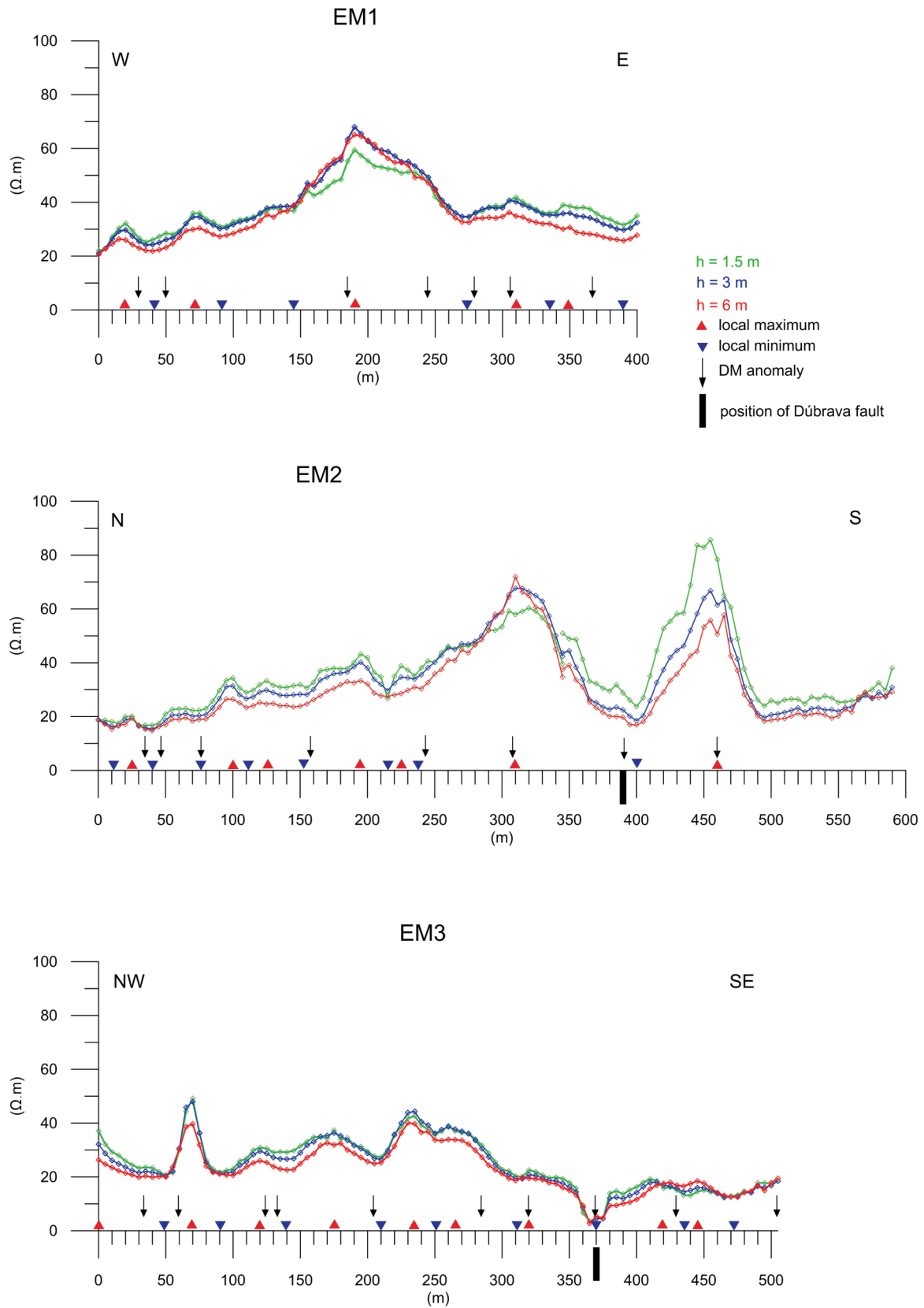
Fig. 2. Results of DEMP measurements on profiles EM1–3 (for location see Fig. 8), with position of local resistivity anomalies and DM response, h is the penetration depth in metres and signs of maxima/minima are denoted with red/blue triangles
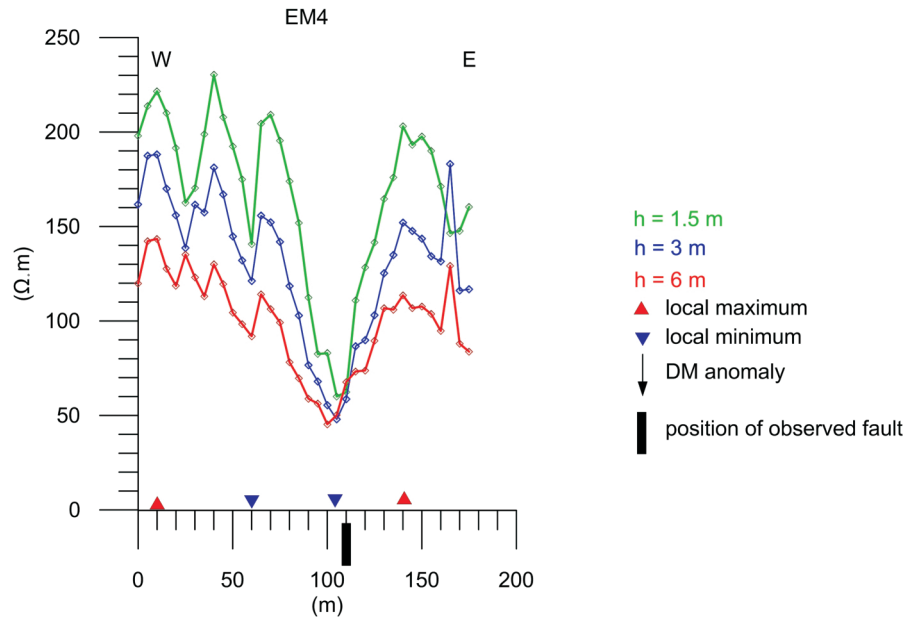
**Fig. 3. Results of DEMP measurements on profile EM4, with position
of local resistivity anomalies and DM response**

rotation stopped. While mapping a discontinuity along its strike the rods rotated as long as the dowser followed the discontinuity trace (Fig. 6). We also employed a pendulum oscillating parallel to a discontinuity trace to identify its strike recorded by DM at a single point. Thus, we were able to map precisely offsets of intersecting faults (cf. Fig. 8).

A map of DM discontinuity traces distinguishes all of the DM fault categories. It delivered a detailed systematic and a regular fault and fracture-zone network, representing appropriately the broader area's regional tectonic style.

Our DM mapping routes did not follow a regular grid. Routes were planned depending on previous results of the route; and on terrain morphology, forest areas, private, cultivated and no-entry areas, as well as other obstacles. All the DM routes and DM points were recorded with a GPS device (Fig. 7).

The DM detection was routinely performed by a single person (M. Dyda), and therefore the acquired data is homogeneous in quality, with mutually comparable observations. The instantaneous DM signal provides localization within a few decimetres. In repeated mapping routes, the operator recorded the same dowsing signals. We thus confirmed that DM observations are reproducible, and it reinforced the reliability of the DM mapping. We continually recorded the same DM signals at the same places in repeated dowsing runs. In addition to M. Dyda's provision of our DM indications, K. Rozimant was also able to record dowsing signals, and his results were well-consistent with those of M. Dyda. The measurements were repeated in the following ways:

– immediately during the tracing, as the dowser crossed fault-discontinuity boundaries several times to confirm anomalies;
– as repetitions after a few days;
– after a few months;
– in some cases even a year later.

In Figure 8, our array of DM discontinuities depicts rock discontinuities reliably detected by dowser. Therefore, our DM signals determine permanent disturbances in natural physical fields from these bedrock discontinuities. In addition, no underground anthropogenic objects were expected in the study area.

RESULTS

The combination of the pragmatic dowsing skills and modern geophysical methods applied to fault detection, resulted in the elaboration of a field mapping procedure. Such an approach enabled us to recognize and localize traces of discontinuities, and the subsequent geophysical measurements confirmed and specified the nature of our dowsing. It resulted in compilation of a detailed map (approximately 1.4 km^2) of faults and other discontinuities with consequent broad utilization (Fig. 8). The map shows the fault arrangements and age relationships of detected discontinuities – offsets of intersecting faults. The distribution of seven geophysical and five radon emanometry profiles with location of important anomalies is also highlighted herein.

The ENE–WSW or E–W trending discontinuities appear dominant. These generally lie parallel to the lithological and tectonic boundaries of Mesozoic units, depicted in Figure 1. Some of DM faults may be lithological boundaries in the bedrock, and later activated as dislocations. Their surface orientation is steep and almost vertical, so our structural map shows a subvertical Sološnica fault zone (SFZ) named after the nearby situated village, segmented by N–S and NW–SE faults (Fig. 8).

Faults identified at the Hrabník pit tested the reliability of our DM and geophysical mapping. The actual, observed fault structures at the Hrabník open mine were consistently recorded by DM mapping, and the fault traces localized by DM coincided with these faults. Four map-scale fault structures were recognized there; three of these were at the recently active mine-face (Fig. 9C–E), and the fourth one forms the Dúbrava fault (Fig. 9A). Due to reclamation processes, the attitude of this latter, was taken from archival data.

The Dúbrava fault identified by DM mapping was also recorded in the EM2 and EM3 geophysical profiles in Figure 2. This fault has a thick fault damage-zone filled with fault rock – strongly squeezed-and-sheared tectonic breccia (Fig. 9B). In addition, the excellent coincidence of the map-scale fault trace with the DEMP negative anomaly was recorded in geophysical profile EM4 (Fig. 3). This identical fault-trace was also captured by DM mapping.
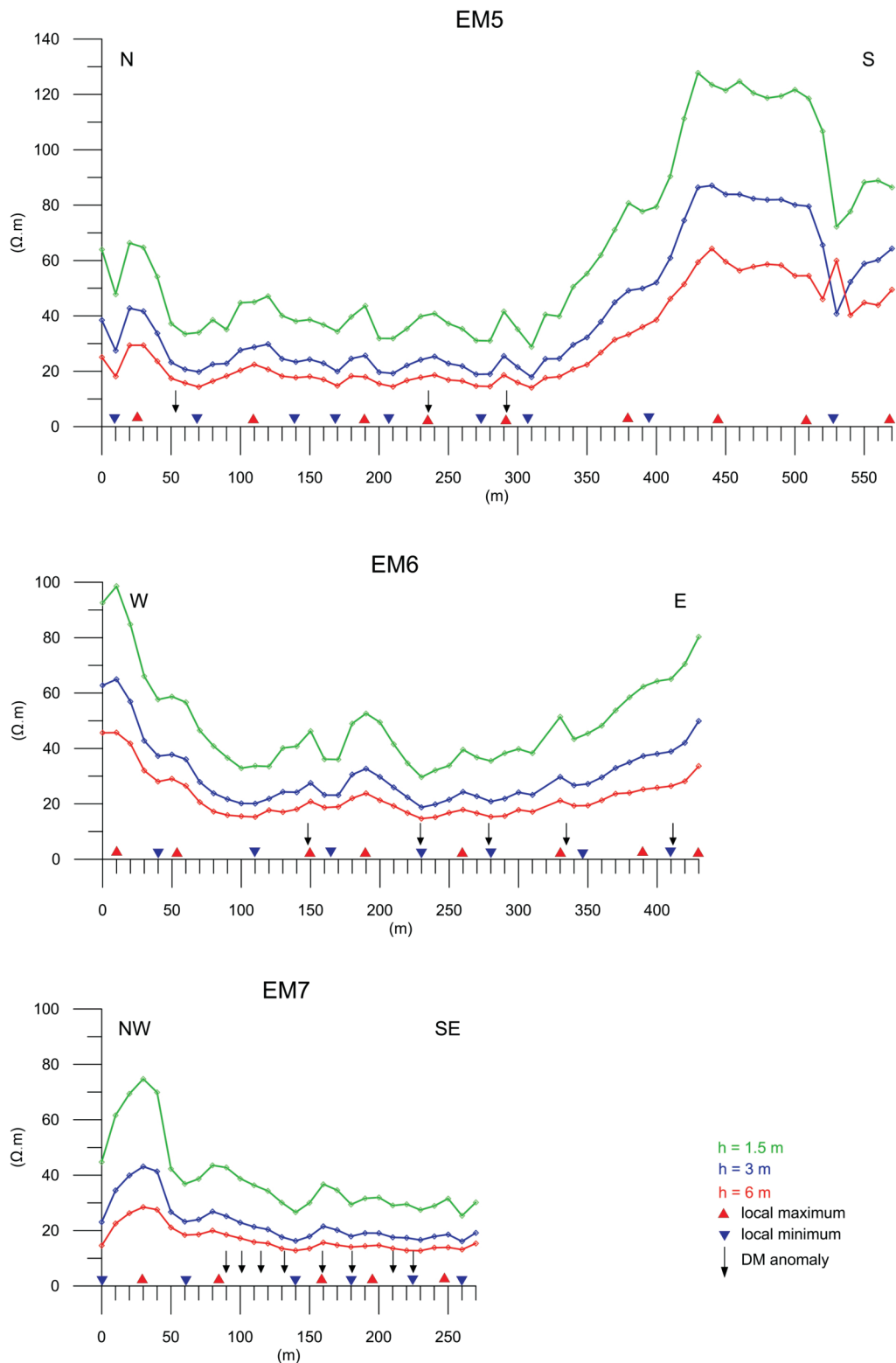
Fig. 4. Results of DEMP measurements on profiles EM5–7, with position of local resistivity anomalies and DM response

The anticipated coincidence of DM faults with DEMP and Rn anomalies was evident in geophysical data; with 87 electromagnetic and 39 DM anomaly indications co-existent. Of these, 25 (64% of DM anomalies) were identical; divided into 23% at maximum electric resistivity sites and 41% at minima (Figs. 2–5). These 25 dowser`s indications covered 9 local electric re-sistivity increases and 16 decreases (Fig. 10). While DEMP anomalies may be positive or negative, with local increase or decrease in electric resistivity, DM indications simply exist or are absent.

We suppose that the sites with decreased electric resistivity indicate faults under extension, and those with the increases
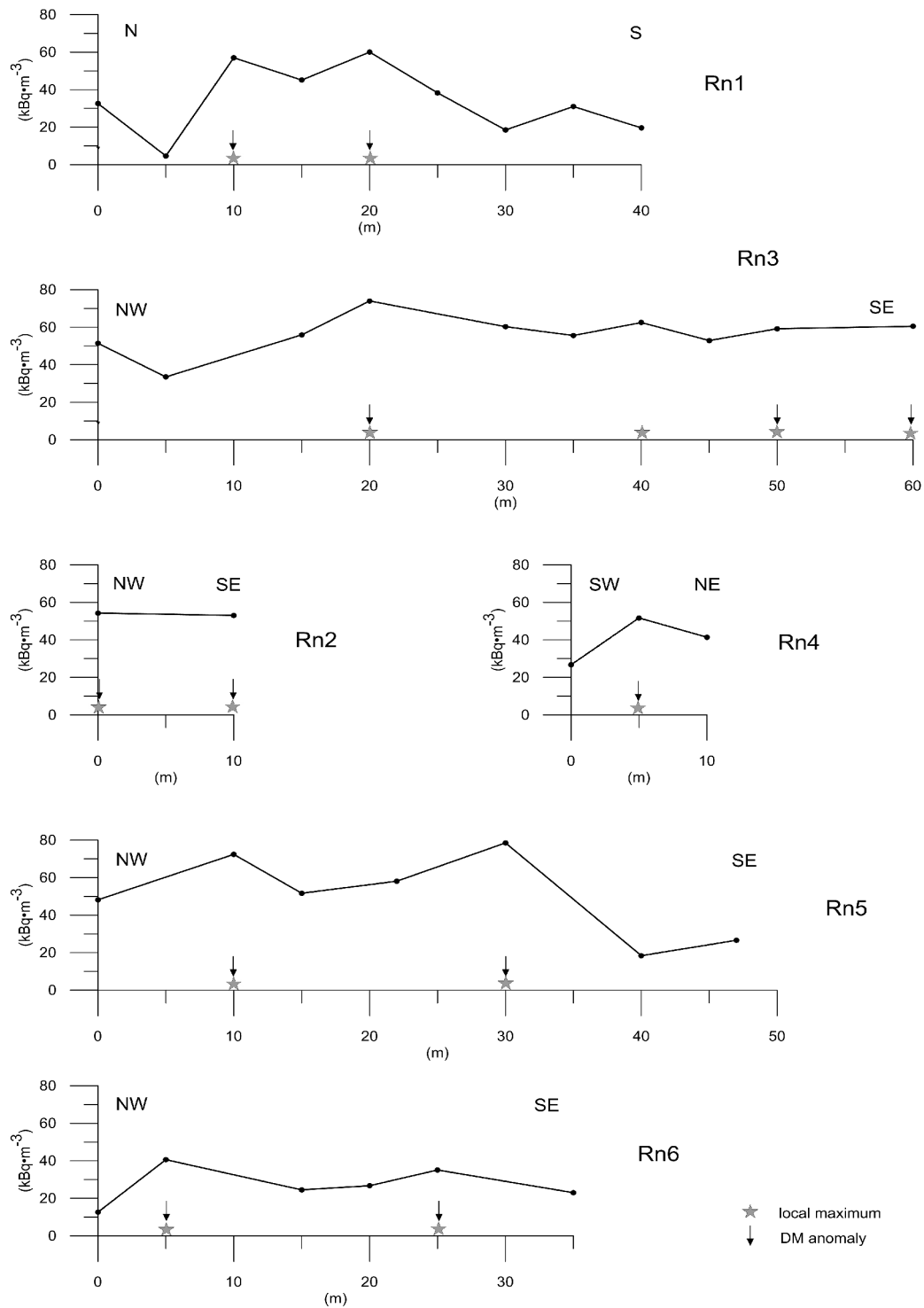
**Fig. 5. Results of radon emanometry measurements on profiles Rn1–6
(for location see Fig. 8), with position of anomalies and DM response**

signify faults under contraction. Here, 36% of DM indications fell within the expressive curve of electric resistivity rather than in the electric resistivity anomaly (Fig. 10). Furthermore, DM indication was never recorded in any constant part of electric resistivity profiles. Almost all the dowser's indications were confirmed by geophysical measurements.

Soil radon (^{222}Rn) emanometry measurements were performed to support the localization of expected tectonic fault zones. Here, a higher radon content in air-sampled soil is detected at 0.8 m depth in the soil horizon because it rises more easily through fractured rock environments inside and along the fault zone. Six short 10–60 m profiles were measured crossing
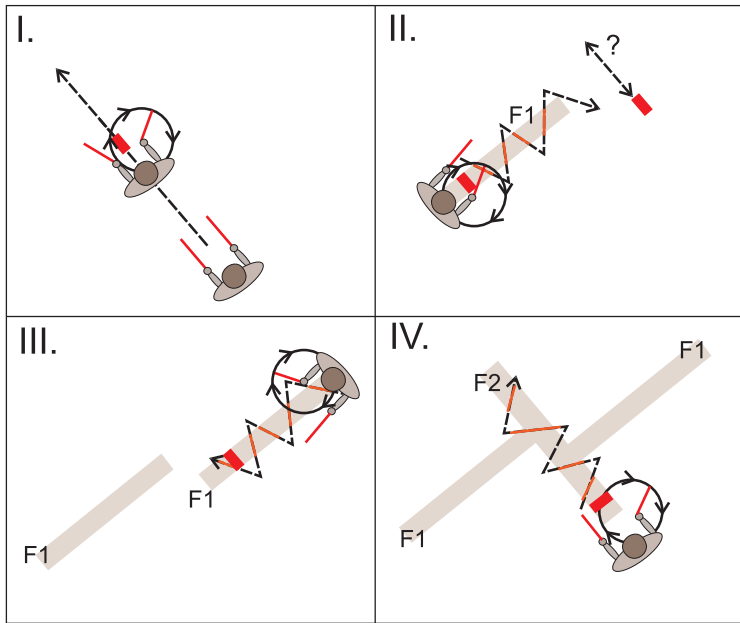
**Fig. 6. Localization of faults
by dowsing mapping procedure**

I – dowser walks in the chosen field direction until the L-shaped virgulas begin clockwise rotation; thus indicating an active zone. Red bar indicates the width of the active zone – a discontinuity, within which the rods are maintaining their rotation. **II** – discontinuity (F1) direction is then mapped by zigzagging its course along the fault strike. As the biodetection signal is lost during advancement along the fault line, a crosscutting fault (F2) may be expected for F1 termination (due to tectonic amputation). The dowser then redirects the route to record the position of the shifted F1 fault segment. **III** – shifted F1 segment is mapped by zigzagging its course. When the biodetection signal is lost during advancement along the fault line, we gain the second point of crosscutting fault F2. **IV** – occurrence of F2 fault line is then confirmed and mapped by zigzagging its course
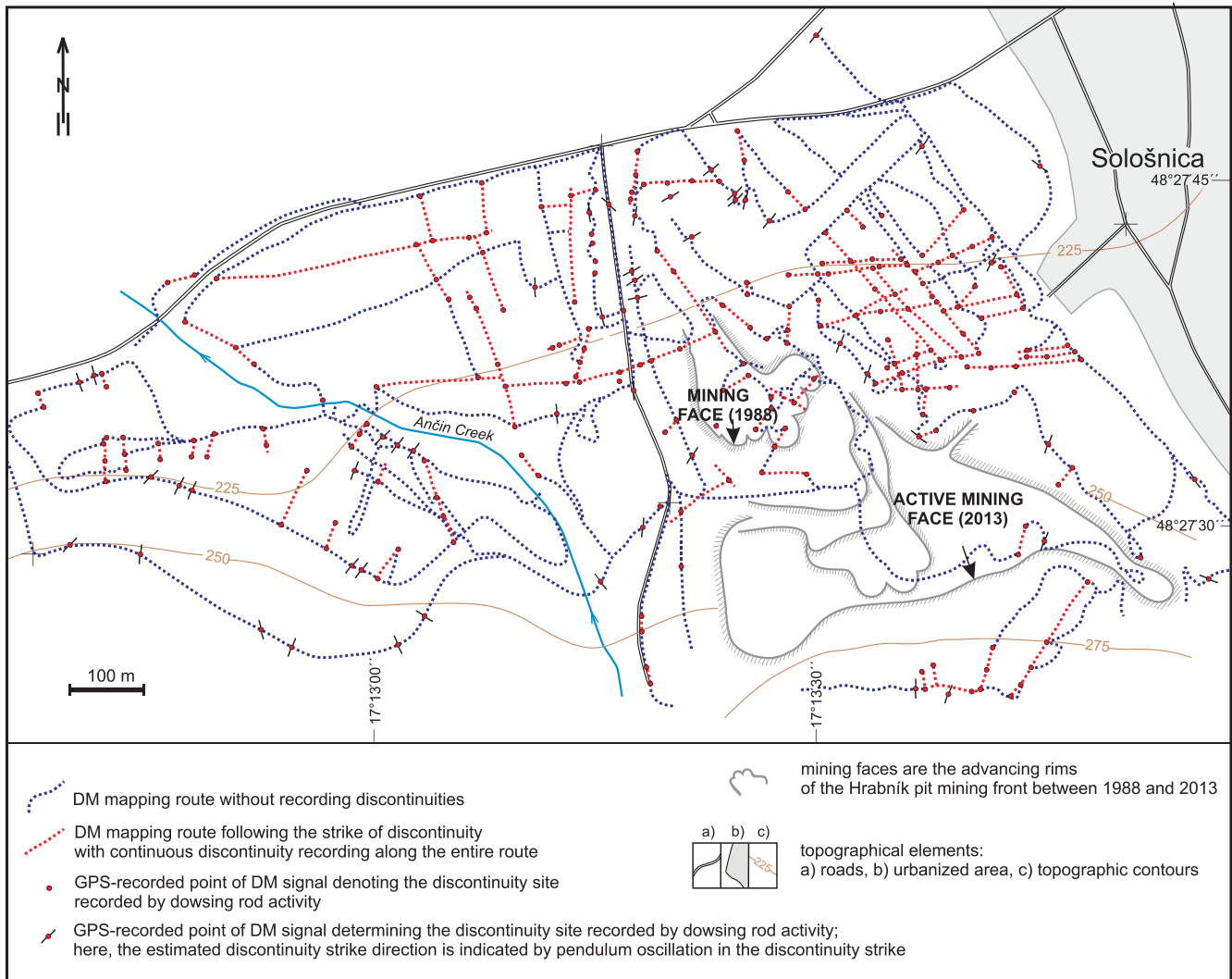

Fig. 7. The network of dowsing method mapping routes in the Hrabník open pit and its surroundings
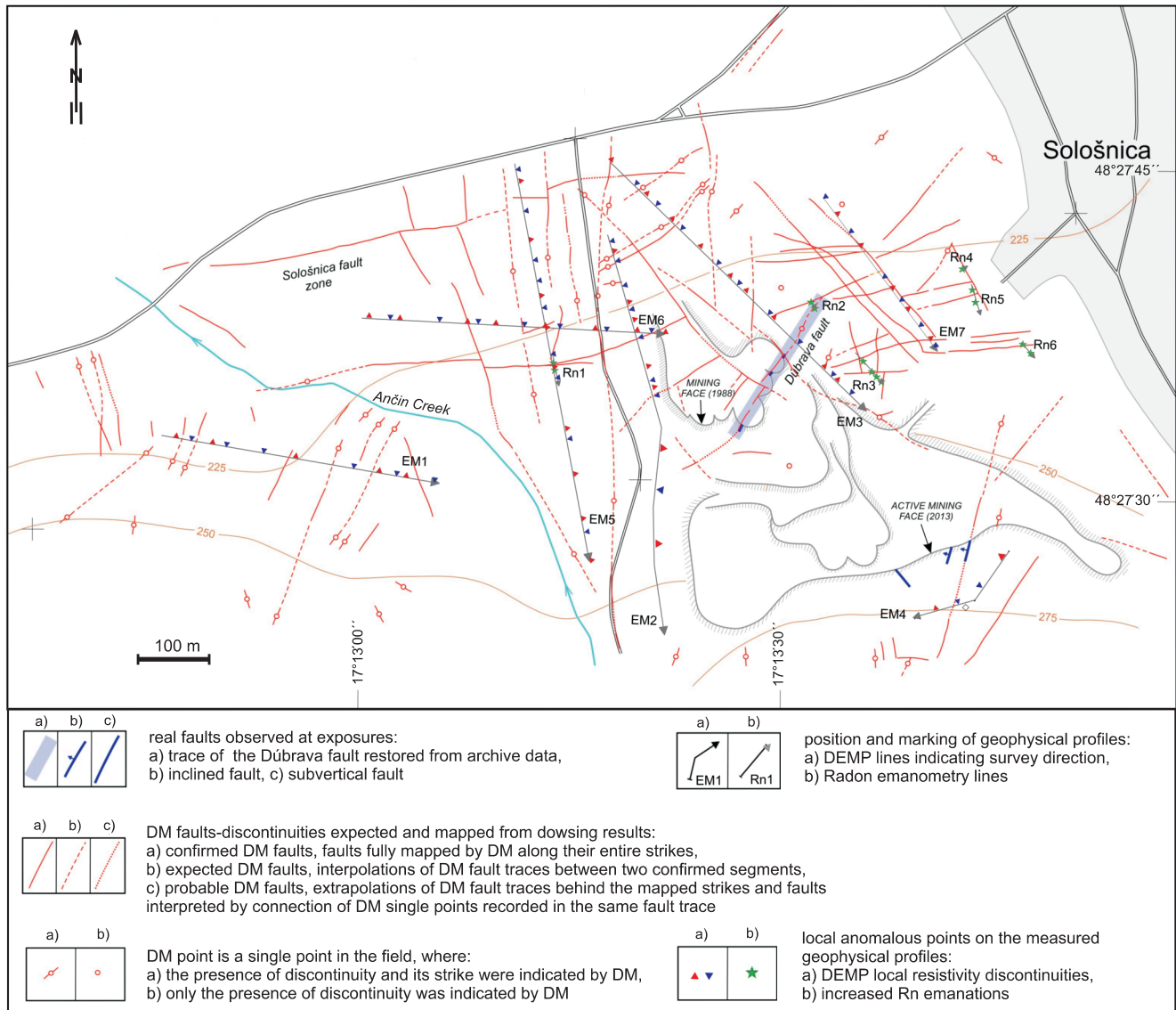
Fig. 8. Legend:

real faults observed at exposures:
a) trace of the Dúbrava fault restored from archive data,
b) inclined fault, c) subvertical fault

DM faults-discontinuities expected and mapped from dowsing results:
a) confirmed DM faults, faults fully mapped by DM along their entire strikes,
b) expected DM faults, interpolations of DM fault traces between two confirmed segments,
c) probable DM faults, extrapolations of DM fault traces behind the mapped strikes and faults interpreted by connection of DM single points recorded in the same fault trace

DM point is a single point in the field, where:
a) the presence of discontinuity and its strike were indicated by DM,
b) only the presence of discontinuity was indicated by DM

position and marking of geophysical profiles:
a) DEMP lines indicating survey direction,
b) Radon emanometry lines

local anomalous points on the measured geophysical profiles:
a) DEMP local resistivity discontinuities,
b) increased Rn emanations

Fig. 8. Map of discontinuities with location of geophysical profiles in the Hrabník open pit and its surroundings

For other explanations see Figure 7

the presumed fault lines (Fig. 8). Detailed measurement of soil radon (^{222}Rn) volume activity (kBq · m^{-3}) along these profiles is presented in Figure 5.

The 40–80 kBq · m^{-3} maximum measured range confirms a tectonic origin of Rn maxima, because "normal" values for this litho-geochemical unit of Paleogene claystone in the Hrabník Formation are between 5–27 kBq · m^{-3} (Daniel, 1999). It is evident in Figure 8 that the near-surface position of the DM tectonic line clearly has the highest radon activity in soil air. This is indicated in a single position on profiles Rn4 and Rn2, two on Rn6, Rn5 and Rn1, and four on Rn3. Multiple maxima indicate several parallel tectonic lines in one tectonic zone.

These anomalies recorded by radon emanometry correlate well with DM faults, and all profiles indicate increased Rn at intersections with DM faults, and in close proximity to expected fault traces.

DISCUSSION

An important argument supporting the reliability of dowsing method for mapping faults is regularity (systematic array) of the gained network of discontinuities, and repeatability of dowsing indications.

However, some questions have emerged during our research. For example, why some distinctive DM discontinuities do not exactly coincide with geophysical curve peaks, but are shifted. It may be due to fault plane inclination, because geophysical and dowsing records may emanate from different depths. Concerning it, we expect combined DM and DEMP testing of well-documented structural faults with known 3D orientation to lead to the development of methodology focused on identifying fault inclination.

Fig. 9. Photo-documentation from the Hrabník pit

A – NE view to the lowermost exploration berm of the Hrabník pit with active mining face in summer 1988 (see Fig. 8); the Sološnica church tower and Plavecký hrad castle ruins are behind; **B** – fault rock from the Dúbrava fault damage zone; lensoidal sandstone fragments are deformed and transposed in the strongly sheared claystone matrix; **C** – currently active mining face of the Hrabník excavation pit; two faults shown in our map on Figure 8 are exposed at the mining face; **D** – details of the fault in Figure 9C: the apparent normal fault (fault surface was not observed), with attitude ca. 280°/75°, with distinctive normal block separation, throw is ca. 2 metres; Upper Oligocene rocks of the Buková furrow basin (alternating poorly indurated sandstones and claystones with S_o ca. 135°/40°) are faulted; **E** – details of the fault in Figure 9C: an oblique-slip fault with attitude ca. 240°/90°; the striae pitch is approximately 40° to the south; fault separation caused no visible offset at the mining face because the striae are parallel with bed dip; **F** – geophysicist (VG, with DEMP instrument) and dowser (MD, with dowsing rods); the mapped terrain and village of Sološnica are behind
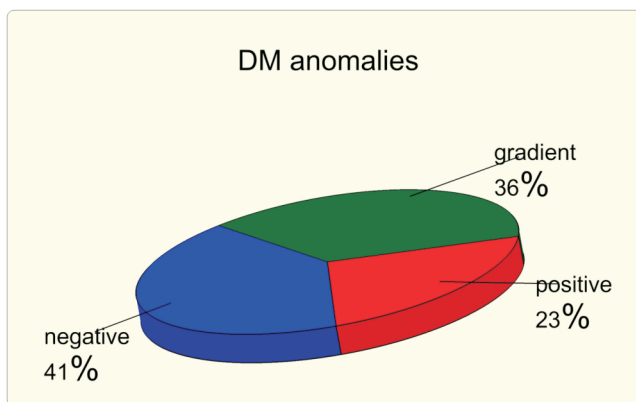
Fig. 10. Percentage correlation of DM anomalies with various DEMP anomalies

Some geophysical anomalies in the study area were not found with the DM method. It is assumed that these anomalies are tectonic structures or lithologies beyond the dowser`s sensitivity. Nevertheless, in many cases, DM seems to appear more sensitive than geophysical measurements, and for faults, it also records discontinuities with low contrast in the physical properties of fault-wall rocks.

There are no mutual shifts at intersection of DM faults in some cases, for example between profiles EM3 and EM7 (Fig. 8). To explain it, we have several options:

i – two discontinuities are vertical faults, and separation along a younger fault crosscutting the older one is dip-slip;

ii – separation along a younger fault is too moderate to be expressed in the map of given scale;

iii – younger discontinuity is not a fault *sensu stricto*, but a fracture or a joint zone with negligible fracture-parallel slip;

iv – both crosscutting discontinuities are joint-fracture zones, or a joint zone cutting lithological anisotropy.

We have found that the Dúbrava fault is a part of a large-scale ENE–WSW Sološnica fault zone (SFZ) rimming the southwestern edge of the Buková furrow basin. In a regional tectonic context, SFZ creates the southern boundary of the Carpathian Shear Corridor (CSC). We expect its ENE–WSW continuation westerly to the Vienna Basin and easterly as the Kátlovce and Rišňovce faults, with its furthermost extension as the Hron morpho-lineament (Pospíšil et al., 1986; see Fig. 1). Beidinger and Decker's (2011) alternative suggestion is that the southern boundary fault of our CSC in the Malé Karpaty Mts. is a curved northern continuation of the NE–SW Litava (Leitha) fault extending along the Pieniny Klippen Belt further to the north and eventually reaching the Outer Carpathians.

CONCLUSIONS

Standard geophysical measurements combined with non-conventional dowsing field survey enabled effective map compilation of faults and other discontinuities in an area where geo-logical-structural mapping failed due to lack of outcrops (Fig. 8). Initial dowsing resulted in a preliminary construction of a detailed map of discontinuities, and geophysical survey then focused on the dowser's selected sites and confirmed the existence of expected discontinuities.

Dipole electromagnetic method was effective and appropriate for locating faults reaching the Earth surface. It was further supported by radon emanometry measurements (Figs. 2–5). High coincidence was established between DM data and geophysical data, where almost all discontinuities identified by DM mapping were also recorded in geophysical results. Here, 64% of DM faults coincided with resistivity anomaly (positive and negative) locations and the remainder correlated with gradient segments of curves (Fig. 10). Radon emanometry profiles, located by our DM faults map, also confirmed the existence of discontinuities determined by dowsing with the maximum values of ^{222}Rn volume activity in soil air (Fig. 5).

The reliability and consistency of DM mapping and geophysical measurements was checked against real observed tectonic faults, and each fault recorded by DM was subsequently identified by geophysics.

Applying the above survey approach, we have mapped the Sološnica fault zone segment buried under the Quaternary cover in precise detail. This faults-array detection can be utilized in geological and various other studies; including palaeo-stress analysis, geological map updating, mining exploitation, urban planning focused on health risk assessment, archaeological research and others.

Finally, we emphasize and recommend DM as the first step in field research, because it focuses on rapid detection of discontinuities. This is an effective tool providing accurate initial evaluation of fault arrays in investigated areas. Our approach simplifies localization in other scientific and technical exploration fields, including geophysics, geochemical sampling and drilling. Moreover, it facilitates and confirms geophysically mapped dislocations in the most suspected and critical parts of the field; thus saving both time and expense.

Dowsing data provides information on various natural phenomena, such as faults, joints, fracture zones, lithological boundaries, water-rich zones and ore-sealed zones, as well as anthropogenic adjuncts including e.g. electric cables and pipes. Therefore, close cooperation with geophysics is essential. We recommend a reconnaissance DM mapping combined with relevant geophysical measurements (Fig. 9F) as a reliable tool in field exploration, construction activities and large building projects. These latter especially include tunnelling, highway and dam construction, ore prospecting and dangerous waste-deposit planning.

REFERENCES

Beidinger, A., Decker, K., 2011. 3D geometry and kinematics of the Lassee flower structure: implication for segmentation and seismotectonics of the Vienna Basin strike-slip fault, Austria. Tectonophysics, **499**: 22–40.

Betz, H.D., 1995. Unconventional water detection. Field test of dowsing technique in dry zones: part 2. Journal of Scientific Exploration, **9**: 159–189.

Born, I.A., 1774. Briefe über Mineralogische Gegenstände, auf seiner Reise durch das Temeswarer Bannat, Siebenbürgen, Ober- und Nieder-Hungarn, Frankfurt a/Main Leipzig, Briefe: 1–22.

Daniel, J., 1999. Geophysical factors of an environment. A natural radioactivity (in Slovak). MŽP SR, Uranpress, Spišská Nová Ves, unpublished report.

Daynes, J., 2012. The Dowsing and Geophysics Project at Moistown, Broadwoodkelly. Interim report 2012, ACE Archaeology Club, Great Britain.

Fiddick, T., 2011. Dowsing: With an Account of Some Original Experiments. The Cornovia Press, Sheffield, United Kingdom.

Giammanco, S., Imme, G., Mangano, G., Morelli, D., Neri, M., 2009. Comparison between different methodologies for detecting radon in soil along an active fault: the case of the Pernicana fault system, Mt. Etna (Italy). Applied Radiation and Isotopes, **67**: 178–185.

Grecula, P., Bartalský, J., Cambel, B., Herčko, I., Kaličiak, M., Matula, M., Melioris, L., Polakovič, D., Slavkay, M., Sombathy, L., Šefara, J., 2006. History of geology in Slovakia (in Slovak). Štátny geologický ústav Dionýza Štúra, Bratislava.

Gruntorád, J., Mazáč, O., 1994. Impact of subtle dynamic geofactors on environment. Acta Universitatis Carolinae Environmentalica, **8**: 3–53.

Janků, J., Pospíšil, L., Vass, D., 1984. A contribution of remote sensing methods to the knowledge of the Western Carpathians geological structure (western segment) (in Slovak). Mineralia Slovaca, **16**: 121–137.

Kowalski, W.C., 1996. Dowsing and radiesthesia; to test or not to test, that is the question (in Polish with English summary). Przegląd Geologiczny, **44**: 39–42.

Landa, V.E., Kovalevsky, A.L., 1997. Integration of dowsing with biogeochemical and electrical prospecting techniques at gold ore deposits. Bulletin of Dowsing, **8**: 9–12.

Lohmann, H.H., 1998. Dowsing versus geophysics. Bulletin for Applied Geology, **3**: 199–203.

Maheľ, M., 1969. Faults and their role in the Mesozoics of the Inner Carpathians (in Slovak). Geologické práce, Správy, **47**: 7–29.

Maheľ, M., Kamenický, J., Fusán, O., Matějka, A., 1967. Regional geology of the ČSSR (in Czech). Nakl. ČSAV Praha.

Marko, F., 2012. Cenozoic stress field and faulting at the northern margin of the Danube basin (Western Carpathians, Slovakia) (in Slovak with English summary). Mineralia Slovaca, **44**: 213–230.

Marko, F., Kováč, M., 1997. Folded Kiscellian turbidites – the evidence of dextral wrenching within ENE-WSW striking shear zone (Hrabník, Malé Karpaty Mts., Western Carpathians). AAPG Bulletin, **81**: 1398.

Marko, F., Kováč, M., Fodor, L., Šútovská, K., 1990. Deformation and kinematics of the Miocene shear zone in the northern part of the Malé Karpaty Mts. (Buková furrow, Hrabník formation) (in Slovak with English summary). Mineralia Slovaca, **22**: 399–410.

Marko, F., Dyda, M., Kóša, J., Silva, A.M., Daudi, E.X.F., Sénvano, A.S., Tembe, S.S., Machado, G., 2006. Hydrogeological environment of the Lebombo monocline (Province Maputo). Abstract volume, 21st Colloquium on African Geology, 03-06 2006 Maputo: 363–364.

Marko, F., Túnyi, I., Andriessen, P.A.M., Fojtíková, L., Piovarči, M., Králiková, S., 2013. Carpathian Shear Corridor – a zone of blocks uplift, tilting, rotation and recent seismic activity (Western Carpathians). GEEWEC2013 "Geological evolution of the Western Carpathians: new ideas in the field of inter-regional correlations", Smolenice, Slovakia, October 16.–19.2013, Abstract Book, (ISBN 978-80-971442-5-8): 59–60.

Michalík, J., 1984. Some remarks on developmental and structural interpretation of the Northwestern part of the Malé Karpaty Mts. (Western Carpathians). Geologický Zborník, Geologica Carpathica, **33**: 481–507.

Moldovan, I.A., Apostol, A., Moldovan, A., Ionescu, C., Placinta, A.O., 2013. The biolocation method used for stress forecasting in Vrancea (Romania) seismic zone. Romanian Reports in Physics, **65**: 261–270.

Plašienka, D., 1990. Regional shear and transpression zones in the Tatric unit of the Malé Karpaty Mts. (in Slovak). Mineralia Slovaca, **22**: 55–62.

Polák, M., Plašienka, D., Kohút, M., Putiš, M., Bezák, V., Filo, I., Olšavský, M., Havrila, M., Buček, S., Maglay, J., Elečko, M., Fordinál, K., Nagy, A., Hraško, Ľ., Németh, Z., Ivanička, J., Broska, I., 2011. Geological map of the Malé Karpaty Mts. region in scale 1:50 000 (in Slovak). MŽP SR, Štátny geologický ústav Dionýza Štúra, Bratislava.

Polák, M., Plašienka, D., Kohút, M., Putiš, M., Bezák, V., Maglay, J., Olšavský, M., Havrila, M., Buček, S., Elečko, M., Fordinál, K., Nagy, A., Hraško, Ľ., Németh, Z., Malík, P., Liščák, P., Madarás, J., Slavkay, M., Kubeš, P., Kucharič, Ľ., Boorová, D., Zlínska, A., Síráňová, Z., Žecová, K., 2012. Explanations to geological map of the Malé Karpaty Mts. region in scale 1:50 000 (in Slovak). MŽP SR, Štátny geologický ústav Dionýza Štúra, Bratislava.

Pospíšil, L., Nemčok, J., Graniczny, M., Doktór, S., 1986. A contribution of remote sensing methods to identification of faults with lateral movements in the area of the Western Carpathians (in Czech). Mineralia Slovaca, **19**: 385–402.